Tellus (1997), 49B, 159–171
Printed in UK – all rights reserved

TELLUS
ISSN 0280–6509

Formation of particulate MSA: deductions from size distribution measurements in the Finnish Arctic

By VELI-MATTI KERMINEN*, MINNA AURELA, RISTO E. HILLAMO and AKI VIRKKULA
Finnish Meteorological Institute, Air Quality Research, Sahaajankatu 20E, FIN-00810 Helsinki, Finland

(Manuscript received 5 January 1996; in final form 10 October 1996)

ABSTRACT

Formation of particulate MSA was studied by conducting a field campaign in the Finnish Arctic. Based on continuous mass size distributions extracted from impactor measurements, 4 MSA modes were identified: an accumulation mode centered between 0.3–0.5 μm of particle aerodynamic diameter, an Aitken mode below 0.1 μm, and 2 supermicron modes that peaked at 2–3 and 7–10 μm, respectively. The lower supermicron mode resulted primarily from the reaction of gaseous MSA with sea salt particles, and the upper mode probably from its reaction with soil-derived particles. From 70 to 90% of the MSA was found in the accumulation mode, where it was distributed very similarly to ammonium. The overall MSA to nss-SO_4^{2-} ratio, R, ranged from 2 to 34%, with most of this variation resulting from different degrees of anthropogenic perturbation in the measured air masses. When comparing different-size particles, R was clearly the highest in the Aitken mode, suggesting that MSA and sulfate contribute with comparable magnitudes to nuclei condensational growth at high latitudes during the summer. The evident variation of R with particle size, together with potential enhanced MSA production in air influenced by pollution, demonstrate further that one needs to be extremely careful when using observed MSA to nss-SO_4^{2-} ratios for estimating the contribution of biogenic sources to total particulate sulfate in different environments. Strong indications on the saturation of MSA over accumulation-mode particles were found. The saturation effect was hypothesized to explain, in part, the observed large partitioning of MSA in the supermicron mode in warm and very acidic aerosol systems. The distribution of submicron MSA, including potential saturation, was shown to be affected significantly by cloud processing.

1. Introduction

The recognized climatic role of sulfate particles has drawn attention to both natural and anthropogenic sulfur compounds, and to their relative significance in regional and global sulfur cycles (Charlson et al., 1987; Penner et al., 1994). The primary source of biogenic sulfur are the oceanic emissions of dimethylsulfide (DMS) to the atmosphere (Andreae and Raemdonck, 1983). Atmospheric DMS is oxidized rapidly to other compounds, the most important of which are SO_2, sulfuric and methanesulfonic acid, dimethylsulfoxide (DMSO), and dimethylsulfone ($DMSO_2$).

For methanesulfonic acid (MSA), no sources other than the oxidation of DMS are known to exist. Because of this, MSA has widely been used for estimating the contribution of biogenic sources to the total sulfate observed (Bates et al., 1992; Li and Barrie, 1993; Heinzenberg and Leck, 1994). Although there seems to be strong coupling between MSA and sulfur-derived particles over remote, southern-hemisphere oceans (Ayers and Gras, 1991), major problems associated with the use of MSA as a tracer for biogenic sulfate still exist. One problem are the uncertainties related to the yield of MSA in the DMS oxidation process;

* Corresponding author.

it is unclear how this yield varies with temperature, or how it depends on various atmospheric pollutants and their concentrations (Bandy et al., 1992; Koga and Tanaka, 1993; Saltelli and Hjorth, 1995).

Another problem is the fact that we do not properly understand processes governing the transport of MSA to the particulate phase where it predominantly is found (Berresheim et al., 1993). Consequently, we cannot reliably predict how MSA is distributed over the particle size range. This makes the comparison between individual measurements quite difficult, especially when different measurement techniques often collect different subpopulations of atmospheric aerosol particles.

In this paper, the formation of particulate MSA is examined. The investigation is based on a field study conducted in the Finnish Arctic during the summer, 1995. The measurement site is exposed to almost clean air from the Arctic seas, to air influenced by different degrees of anthropogenic perturbation, and to air of purely continental origin. The field campaign was performed in the summer because of the high biological activity and resulting strong MSA production over the nearby oceans during that time period.

The principal goal of this work is to elucidate how MSA is transported to particles of different size and type under different ambient conditions. For this purpose, MSA and major inorganic compounds have been measured using a size-classifying impactor sampling. From the impactor data we have constructed continuous mass size distributions of the measured compounds over the range 0.03–15 μm of particle equivalent aerodynamic diameter (EAD). The interpretation of the data is assisted with the use of air mass back trajectories, and by analyzing meteorological and aerosol parameters monitored simultaneously with the impactor sampling.

2. Experimental

2.1. Measurement site

The measurements were carried out at the Sevettijärvi station (69°30′N, 28°50′E) in the northernmost Finland (Fig. 1). The site is located near the Arctic Ocean some 30 km from the closest bay of the Barents sea. The station stands on a small hill some 30 m above the nearby lake surface, and 130 m above the sea level. The surrounding area has numerous lakes and pine- and birch-covered hills, but no high mountains.

The largest nearby pollution sources, situating approximately 60 km south-east of the station, are the industrial areas of Nikel and Zapolyarnui in the Kola Peninsula. Local pollutant emissions are low. There are only 5 houses within a radius of 3 km from the station, and no major population centers within a radius of 40 km. The closest road, 2.5 km from the station, has minor traffic and does not produce any significant disturbances to the measurements.

2.2. Measurements and chemical analyses

The measurements covered 5, 2- to 3-day periods between June and August 1995. These periods were: (1) 5–8 June (17.37–6.50); (2) 8–11 June (8.41–8.20); (3) 14–18 June (10.00–8.00); (4) 10–13 July (16.43–19.00), (5) 15–17 August (5.38–14.49). The numbers in the parentheses refer to the starting and ending times (in UTC) of the sampling, respectively.

Aerosol particles were collected by a Berner low pressure impactor (BLPI; Berner and Lürzer, 1980). The impactor had ten collecting stages and a preimpactor stage removing particles greater than about 15 μm of EAD. The particle cut-off sizes of the stages were 0.035, 0.067, 0.095, 0.17, 0.34, 0.56, 1.1, 2.3, 4.3 and 7.8 μm, respectively, at 980 hPa and 278 K. During the sampling the impactor was in a vertical position, with an inlet (Liu and Pui, 1981) in the top to minimize the effect of wind on the transport efficiency of coarse particles from the atmosphere. The inlet also had a discriminator (based on an impactor with 15 μm cut-off diameter) for large particles and rain droplets. The BLPI was on over the whole sampling periods, and operated at ambient temperature and humidity all the time.

From the impactor samples, water-soluble MSA and major inorganic compounds (SO_4^{2-}, NO_3^-, Cl^-, NH_4^+, Na^+, K^+, Ca^{2+} and Mg^{2+}) were analyzed using an ion chromatography. The overall ionic concentrations given by the impactor were compared with those obtained from a filter device operating approximately over the same sampling periods as the impactor. The particle collection efficiency of the filter device decreased rapidly after some 3–4 μm of EAD.

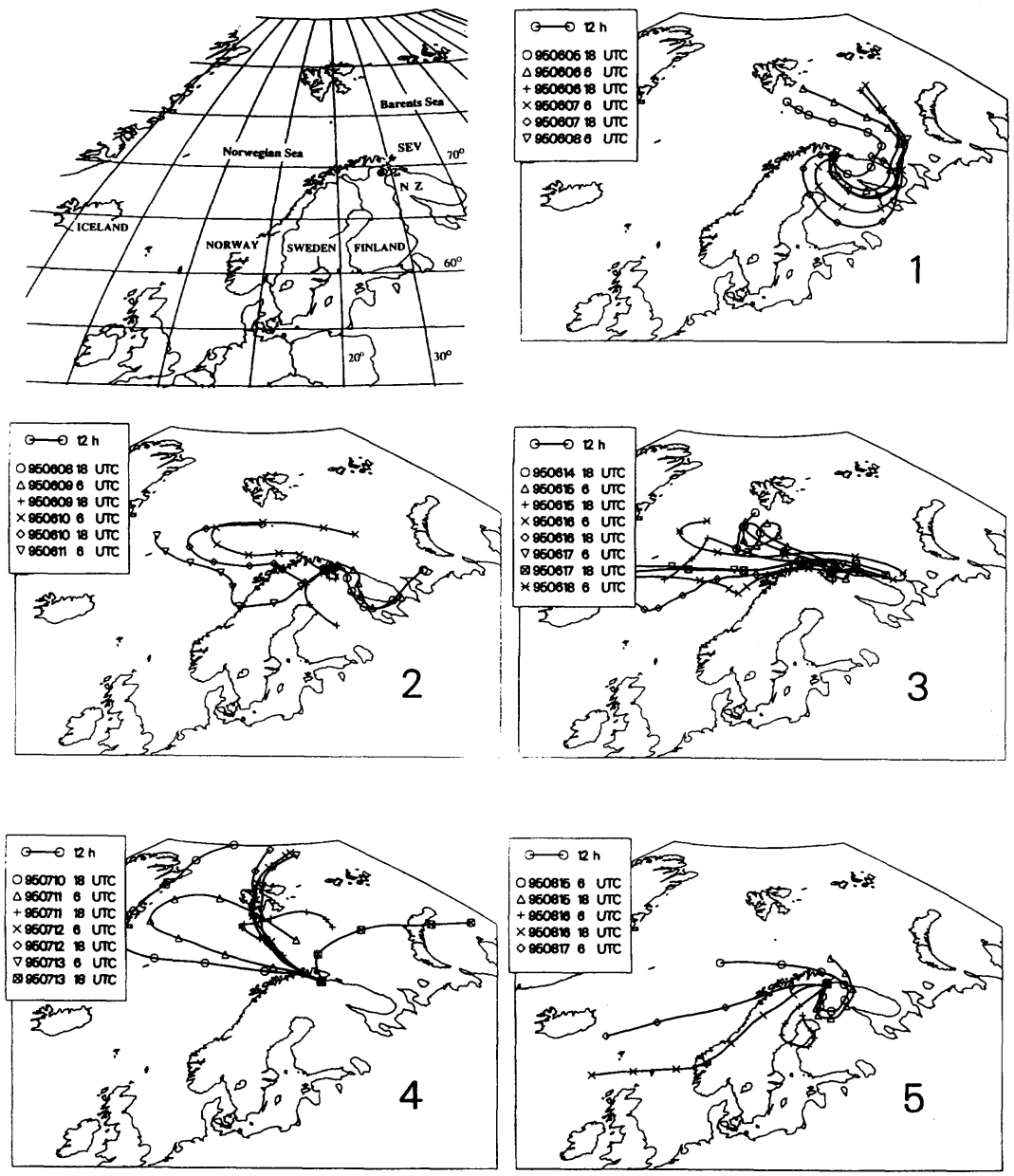

Fig. 1. The location of the Sevettijärvi measurement station (SEV) and of the 2 pollution sources, Nikel (N) and Zapolyarnui (Z), in the Kola Peninsula. Air mass trajectories calculated by TRADOS during the 5 sampling periods are also shown. The dates in the trajectory pictures are in formate (year, month, day, arrival hour).

Concurrent to the impactor measurements, basic meteorological and aerosol parameters were monitored continually. Meteorological parameters included temperature, relative humidity, wind and rain. Concentrations of gaseous SO_2 were monitored using a differential optical absorption spectroscopy (DOAS, Opsis model AR 500), and those of aerosol particles above the 14-nm size using a

Condensation Particle Counter (CPC, TSI model 7610) and over size ranges $0.3 < d_p < 0.5$ and $0.5 < d_p < 2$ μm using a Laser Particle Counter (LPC, TSI model 7430).

3. Results and discussion

3.1. Description of sampling conditions

Fig. 1 illustrates the transport history of measured air during the sampling periods. The three-dimensional, 96-hour back trajectories were calculated using the TRADOS model developed at the Finnish Meteorological Institute (Valkama and Rossi, 1992). During the measurement period #1, observed air masses originated primarily from the Arctic seas. Prior to their arrival at the station, however, these air masses spent 1 or 2 days over the Finland, or over the north-west corner of Russia. The influence of land can be seen in large LPC counts, and in high SO_2 and sulfate concentrations (Tables 1, 2).

The period #2 was exposed to two totally different air masses: those coming from Russia, and those from the Norwegian or Barents Sea. As a result both MSA and sulfate concentrations were quite high. The small ratios of both Na^+ and MSA to nss-SO_4^{2-} highlight the dominance of anthropogenic sources over the marine ones in this sample.

During the period #3, measured air masses originated from the Northern Atlantic or from the Norwegian Sea, and traversed the northernmost coast of Scandinavia prior to their arrival at our site. As shown by Tables 1, 2, an anthropogenic signature is much weaker in this than in the first two samples.

The period #4 was the cleanest one, with air coming rather directly from the Arctic seas. The dominance of Arctic, marine air is evident when looking at the observed temperature range, or measured sulfate, SO_2 and particle concentrations. The MSA to nss-SO_4^{2-} ratio was clearly the highest.

Most air masses during the period #5 originated from the Northern Atlantic or from the Norwegian

Table 1. *The means of selected meteorological and aerosol parameters during the measurement periods # 1–5; also, the ranges, calculated from the 10th and 99th percentiles of the observed data, are given*

Measurement	1	2	3	4	5
T (°C)	14	10	9	6	15
	(8–19)	(6–20)	(6–21)	(5–9)	(10–20)
rh (%)	71	83	71	81	74
	(55–99)	(59–100)	(46–99)	(73–97)	(52–96)
SO_2 (μg m^{-3})	3.5	4.3	1.2	0.2	4.3
	(0.3–110)	(0.1–80)	(<0.1–19)	(<0.1–0.8)	(0.1–150)
CPC (cm^{-3})	3800	2400	2000	200	1400
	(2400–12000)	(570–16000)	(300–8900)	(36–1000)	(620–8600)
LPC (cm^{-3}) (0.3–0.5 μm)	24	12	4.4	0.5	6.5
	(12–39)	(1.5–43)	(1.6–16)	(0.08–1.8)	(1.2–13)
LPC (cm^{-3}) (0.5–2 μm)	1.9	1.4	1.2	0.1	0.7
	(0.8–5.1)	(0.1–5.5)	(0.6–5.2)	(0.03–0.4)	(0.2–2.0)

Table 2. *Concentrations of MSA^- and nss-SO_4^{2-} (ng m^{-3}) in BLPI samples #1–5, together with some concentration ratios*

Measurement	1	2	3	4	5
MSA^-	28	45	42	33	25
nss-SO_4^{2-}	1400	1300	390	96	1000
MSA^-/nss-SO_4^{2-}	0.02	0.03	0.11	0.34	0.02
Na^+/nss SO_4^{2-}	0.13	0.05	1.3	2.2	0.24
SO_2/nss SO_4^{2-}	2.4	3.2	3.1	1.9	4.3

Sea, and had some contact with land over the northernmost Scandinavia and Kola Peninsula. The high peaks in SO_2 concentrations combined with large mean SO_2 to nss-SO_4^{2-} ratio during this period is indicative of captures of relatively fresh emissions, probably from the Kola Peninsula area.

3.2. *Data inversion*

The size distribution data obtained from the BLPI is discrete. In order to resolve the modal structure of various chemical components, the raw BLPI data were run by the inversion code MICRON described in detail by Wolfenbarger and Seinfeld (1990). MICRON turns discrete mass size distributions into continuous form, from which the modal parameters of the chemical components (their mass mean diameter, geometric standard deviation and concentration) can be calculated. For this latter purpose a software developed by Winklmayr et al. (1988) was used.

A successful inversion by MICRON requires information on the impactor collection characteristics and on errors involved. In this work, we had detailed collection efficiency curves for all impactor stages based on the calibrations of Wang and John (1988) and of Hillamo and Kauppinen (1991). The changes that the impactor collection efficiency curves experience due to changes in the ambient temperature were accounted for when performing the inversion.

The errors used as an additional input for MICRON include those from sampling, those from chemical analyses, and those from the inversion itself. Since all these errors were not known quantitatively, we applied a procedure where we ascribed a certain base error (both absolute and relative) to each impactor stage, and then used larger errors if uncertainties in the chemical analyses were larger than that. If the relative errors are less that about 10–20% for the stages, the modal structure of a species' size distribution can usually be resolved pretty well, and the resulting modal parameters are not very sensitive to the exact magnitude of the errors. If the errors are larger, individual modes become broader and flatter (their geometric standard deviation increases), and it becomes more difficult to distinguish between modes that are located close to each other. These kind of situations are relatively easy to identify from inverted data.

The main constituents we were interested in this work are MSA and non-sea-salt sulfate. For both these compounds, the estimated analysis errors were always less than 10% over the accumulation mode, and less than 15% over the supermicron size range. The respective errors over the Aitken mode were generally below 15%, except in measurement #4 having very low Aitken-mode concentrations. At that sample, the errors for MSA in the impactor stage 2 (0.067–0.095 μm), and for sulfate in the stages 1 and 2, were of the order of 50%. The blank concentrations of both MSA and sulfate were below the analytical detection limit.

In general, the inversion preserved the total ionic mass extremely well for the species analyzed in this study. It is expected that the modal parameters are relatively accurate in case of the accumulation mode and, with some reservation, over the supermicron particle size range. Due to the limited size resolution of the impactor and to low mass loadings below 0.1 μm, we could not make reliable estimates concerning the mass mean diameter and the geometric standard deviation of the species' Aitken mode. The concentrations of various species in the Aitken mode can, however, be considered quite reliable for most of the measurements.

3.3. *Distribution of MSA over the particle size range*

The mass size distributions of MSA, non-sea-salt sulfate, and ammonium during the five sampling periods are presented in Fig. 2. In all samples, 4 separate MSA modes can be identified: an accumulation mode centered between 0.3 and 0.5 μm (Table 3), an Aitken mode below 0.1 μm, and two supermicrometer modes centered at 2–3 μm and 7–10 μm, respectively. In sample #1 there was another mode in the accumulation range at around 0.1–0.2 μm. Of MSA mass, 70–90% was located in the accumulation mode, 3–10% in the Aitken mode, and 5–15% and 1–10% in the lower- and upper-size supermicron modes, respectively.

Studies in marine environments have found a close correlation between supermicron MSA and the effective surface area of the sea-salt aerosol (Pszenny, 1992; Huebert et al., 1993). An effective

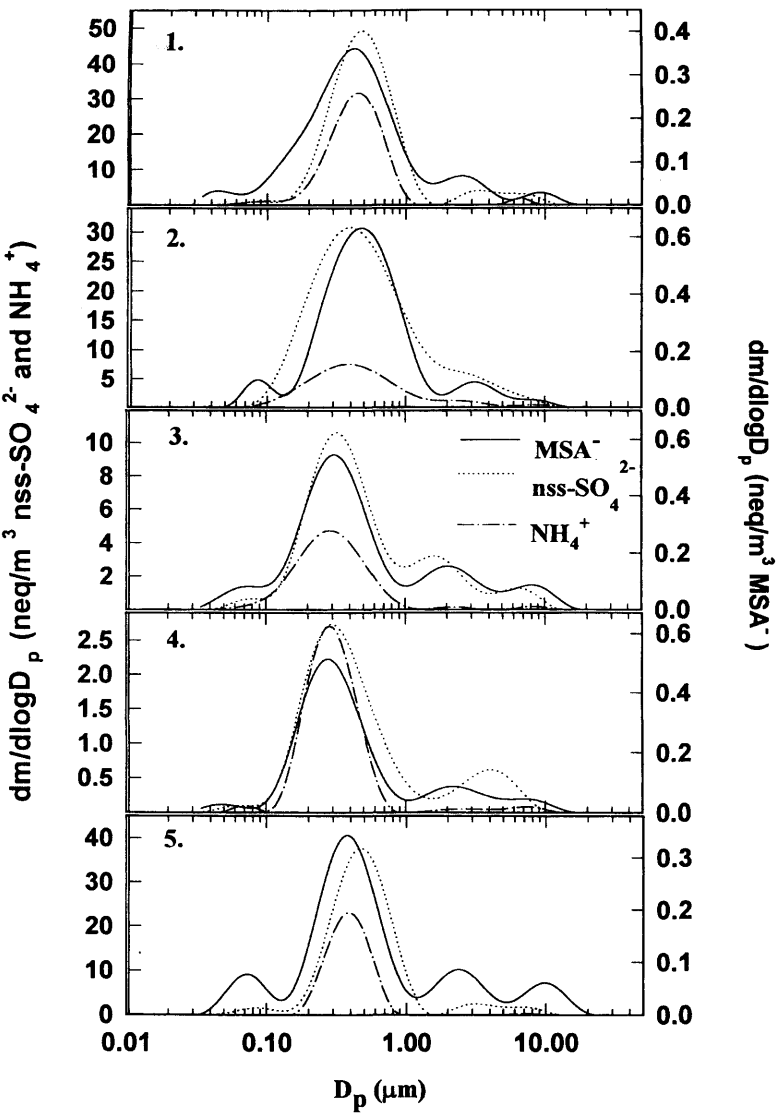

Fig. 2. Mass size distributions of MSA^-, nss-SO_4^{2-} and NH_4^+ in samples #1–5.

surface area lies between the first (diameter) and second (surface area) moment of the particle number size distribution, depending on condensation/reaction kinetics of the condensate on particle surfaces. If, however, the condensate achieves a chemical equilibrium between the gas and particulate phases (saturation), it will, depending on the phase-state of the particles, be distributed between the surface-area and volume moment of the particle number size distribution (Kerminen and Wexler, 1995).

Of the two sea-salt ions in our samples, Na^+ and Mg^{2+}, from 86 to 99% and from 95 to 100% were found in the supermicron particles, respectively. The mass size distributions of both these species peaked at around 4 μm (Table 3), and the respective surface-areas between 2 and 3 μm. The latter size is exactly where the lower-size supermi-

Table 3. *Modal mass mean aerodynamic diameters (μm) of selected species over the accumulation and supermicrometer size ranges; the geometric standard deviations of the modes are given in parentheses*

Measurement	1	2	3	4	5
accumulation:					
MSA	0.44 (1.8)	0.47 (1.8)	0.31 (1.7)	0.28 (1.7)	0.38 (1.6)
nss–SO_4^{2-}	0.48 (1.7)	0.42 (2.0)	0.32 (1.6)	0.31 (1.7)	0.48 (1.6)
NH_4^+	0.44 (1.5)	0.38 (2.0)	0.29 (1.7)	0.29 (1.5)	0.38 (1.4)
supermicron:					
MSA	2.6 (1.5)	3.3 (1.4)	2.1 (1.6)	2.2 (1.6)	2.4 (1.5)
	9.3 (1.3)	8.5 (1.3)	8.1 (1.4)	7.4 (1.5)	9.8 (1.4)
Na^+	2.8 (1.8)	3.2 (1.7)	3.8 (1.8)	3.9 (1.9)	3.8 (1.8)
Mg^{2+}	3.0 (1.9)	3.4 (1.8)	3.8 (1.7)	3.9 (1.8)	3.8 (1.8)

cron MSA mode peaks in samples #3, 4 and 5. It seems very plausible that this MSA mode is due to condensational transport of gaseous MSA into sea-salt particles.

What is the origin of the upper-size supermicron MSA mode? We propose that it results from the reaction of MSA with soil-derived particles. Since elements of purely crustal origin were not analyzed, the only data to support for this hypothesis are the size distributions of nss-Ca^{2+}. The mass mean diameter of nss-Ca^{2+} was greater than that of sea-salt, and it frequently had a tail reaching above 10 μm. Soil particles could explain the observations of Quinn et al. (1993), according to which supermicron MSA was distributed over much broader size range in a continental site than in measurements made over the ocean. In samples #1 and 2, soil particles may have caused the shift of the first supermicron mode to somewhat larger size than the effective surface-area of sea-salt particles.

Submicrometer MSA was predominantly located in a relatively stable-size accumulation mode. Except for sample #2, MSA was distributed very similarly to ammonia over this mode, indicating the same gas-to-particle transport mechanism for these two compounds. This mechanism undoubtedly is condensation. Interestingly, both MSA and NH_4^+ peaked at slightly smaller size than nss-SO_4^{2-}.

The distribution of accumulation-mode MSA in sample #2 can be explained by the arrival of two very different air mass types during the measurement period. The first type came directly from the ocean and probably had most of the measured MSA. The second type contained somewhat smaller particles of predominantly continental origin, and had large amounts of nss-SO_4^{2-} and NH_4^+ with it. The broadness of the accumulation mode supports the hypothesis of two air mass origins.

Until present, little data on MSA in particles smaller than 0.1 μm have been reported. Our measurements revealed a separate MSA mode in the Aitken size range. Because of very low particle mass loadings over the Aitken range, the exact location of this MSA mode cannot be determined. Anyhow, one can see a clear gap between the Aitken- and accumulation-mode MSA, both by looking at the discrete size distribution data and by analyzing continuous MSA size distributions. The gap is probably due to cloud processing, a phenomenon returned later in more detail.

3.4. MSA to nns-SO_4^{2-} ratio

The ratio of MSA to nss-SO_4^{2-}, termed henceforth *R*, has been used in evaluating the contribution of biogenic sources to total sulfate over various geographical locations, and in exploring the relative significance of different DMS oxidation pathways (Berresheim et al., 1991; Li and Barrie, 1993; Heintzenberg and Leck, 1994; Leck and Persson, 1996). Air masses having a strong anthropogenic signature frequently have *R* smaller than 1%. For cleaner air, *R* varies from a few per cent over the equatorial marine environment to near, or even above, 100% at high-latitudes during the summer (Salzman et al., 1986; Bürgemeister and Georgii, 1991; Bates et al., 1992; Savoie et al., 1992; Li et al., 1993). The reason for the evident increase of *R* toward polar regions is not quite

clear, but it has been explained by the latitudinal differences (i) in temperature which affects the MSA yield in the DMS oxidation process, (ii) in perturbations by anthropogenic sulfur emissions, and (iii) in the amount of clouds, which has impacts on the precipitation scavenging of MSA and nss-SO_4^{2-}, and on the potential destruction of MSA in the droplet phase by chemical reactions (Li et al., 1993).

In our samples, the ratio of MSA to nss-SO_4^{2-} ranged from 2 to 34% (Table 2). Since the MSA concentration varied by less than a factor 2 between the samples, most of the scatter in R can be ascribed to different degrees of anthropogenic influence in measured air masses. The impactor data allows us to evaluate how MSA to nss-SO_4^{2-} ratio varies with particle size. In Fig. 3 we have plotted the value of R over the Aitken, accumulation and supermicrometer size ranges. As expected, accumulation-mode R is very similar to that calculated from the overall MSA and nss-SO_4^{2-} concentrations. The supermicrometer R varies qualitatively the same way as the Na^+ to nss-SO_4^{2-} ratio, which is consistent with our earlier speculation of the reaction of MSA with sea-salt particles.

An interesting feature in Fig. 3 are the high MSA to nss-SO_4^{2-} ratios in the Aitken mode compared to larger-size particles, especially in measurements influenced by anthropogenic emissions. A potential reason for this is cloud processing: while both Aitken- and accumulation-mode particles absorb gaseous MSA and sulfuric acid, only accumulation-mode particles convert SO_2 effectively to sulfate in activated cloud droplets. Since from 50 to 90% of the tropospheric

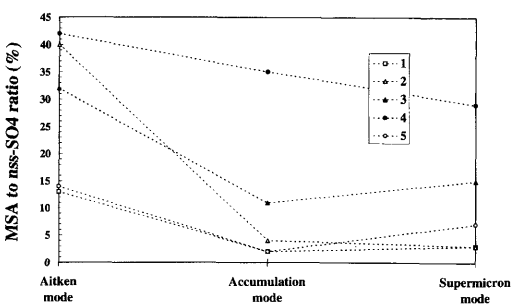

Fig. 3. The MSA^- to nss-SO_4^{2-} ratio over the Aitken, accumulation, and supermicron size ranges in samples #1–5.

sulfate is believed to be produced by clouds (Langner and Rodhe, 1991), the observed difference between the Aitken- and accumulation-mode R is no surprise.

Another reason for the smaller MSA to nss-SO_4^{2-} ratios in the accumulation mode could be heterogeneous oxidation of SO_2 to sulfate on the surface of mostly accumulation-size combustion particles. This phenomenon has frequently been observed in power plant plumes (Newman, 1981), and it could partly explain why the deviation between Aitken- and accumulation-mode R is greater for the pollution-influenced cases than for the clean marine case. A larger set of measurements is, however, needed to confirm this hypothesis.

Our filter measurements which cover the whole summer, as well as data from several other measurements (Watts et al., 1990; Mihalopoulos et al., 1992), indicate that the interaction of marine air with polluted air enhances MSA production. This together with the evident variation of R with particle size demonstrate clearly that one needs to be extremely careful when using observed MSA to nss-SO_4^{2-} ratios in evaluating the contribution of biogenic sources to total particulate sulfate in different environments.

Our observations may also have implications on global cloud condensation nuclei (CCN) production. The theory predicts that MSA is unlikely to participate in new particle production under conditions typical of the marine atmosphere (Hoppel, 1987; Van Dingenen and Raes, 1993). Based on this, it has commonly been believed that MSA does not significantly contribute to CCN production. This may not be the whole truth: it is quite possible that the limiting step for CCN production is the growth of nuclei into the CCN size rather than the nuclei production itself. The high MSA to nss-SO_4^{2-} ratios over the Aitken range indicate that MSA may, under certain conditions, affect nuclei growth almost similarly to sulfate. This should be kept in mind when investigating, for example, the interactions between natural and anthropogenic sulfur emissions, CCN production, and climatic forcing.

3.5. *Cloud processing and submicron MSA formation*

Clouds have large impacts on atmospheric aerosols. They are responsible for the wet deposition

of gases and particles, and for the accumulation of species like sulfate into the particulate phase. Cloud processes change the number, size and chemical composition of particles in the atmosphere. The studies of Hoppel et al. (1994a,b) and Kerminen and Wexler (1995) have shown that processing of air through nonprecipitating clouds moves particles from the upper end of the Aitken mode to the accumulation mode. As a result of this, a gap between these two modes around the minimum droplet activation diameter is created.

The Aitken-accumulation mode gap is evident in most of our samples. This, taken together with much higher MSA to nss-SO_4^{2-} ratio in the Aitken mode, indicate that measured air masses had probably interacted with clouds prior to their arrival at Sevettijärvi. How does the submicron MSA size distribution depend on the interplay between condensational transport of MSA and cloud processing? One can identify four different but not necessarily mutually exclusive gas-to-particle transport routes for submicron MSA: (a) MSA is produced from dissolved DMS in cloud droplets, (b) MSA condenses to the Aitken mode, wherefrom part of it is transferred to the accumulation mode as the Aitken-mode particles grow in size, (c) MSA condenses to cloud droplets and remains in the particulate phase as the droplets evaporate, or (d) MSA condenses directly to accumulation-mode particles during non-cloudy periods.

The studies of Lee and Zhou (1994) show the route (a) to probably be of minor importance in the atmosphere. How about the route (b)? It has been demonstrated that the Aitken mode may serve as a dominant source of accumulation-mode particles in marine environments (Russell et al., 1994; Raes, 1995). The mechanism most likely to turn Aitken-mode particles into accumulation-mode ones is cloud processing, with the next likely one being condensational particle growth. Coagulation is too slow to significantly enhance the size of Aitken-mode particles in the lower-troposphere marine atmosphere (Kerminen and Wexler, 1995). Noting this and the fact that particle number concentrations in the Aitken mode usually are of the same magnitude or greater than those in the accumulation mode, one should find more MSA in the Aitken than in the accumulation mode if the route (b) was important. Since this was not the case, we conclude that accumulation-mode MSA is formed principally via routes (c) or (d).

Let us then analyze the relative importance of the routes (c) and (d). The average concentration of particulate MSA in high-latitude marine boundary layers range from a few ppt to about 20 ppt during the summer (Li et al., 1993; Heintzenberg and Leck, 1994; Jaffrezo *et al.*, 1994; Leck and Persson, 1996). Since an average lifetime of particulate MSA is some 0.5–2 days (Huebert et al., 1993), a gas-phase production rate of $P \sim 0.1$–1 ppt h^{-1} is needed to maintain the observed total MSA concentration. Now, if MSA would condense to particles during cloud stages only (by the route c), the average gas-phase MSA concentration would have to be of the order $P \cdot t_C$, where t_C is the time interval between two successive cloud events. Excluding very cloudy boundary layers, t_C normally is longer than an hour, which would lead to MSA(g) levels greater than 0.1 ppt. This is clearly above measured MSA(g) concentrations of the order 0.01 ppt or less (Eisele and Tanner, 1993; Berresheim et al., 1993). We conclude that most MSA is transported to particles in a cloud-free air (by the route d), not during cloud events. The situation may, however, be different for precipitating or otherwise very cloudy boundary layers.

As mentioned earlier, condensation of a species to a stable-size mode without any saturation effects distributes it according to the effective surface area of the mode. In our samples, MSA was distributed over the accumulation mode rather similarly to sulfate, a compound that is expected to be distributed close to the volume moment of this mode. Does this conflict with our speculation on how accumulation-mode MSA was formed? The seeming discrepancy can be explained by (1) the possible inaccuracies in the data, (2) the saturation of MSA with respect to the accumulation mode, or (3) cloud processing of accumulation-mode particles.

The first option is unlikely: although both chemical analysis and data inversion generate uncertainties in modal parameters, our earlier experiments have demonstrated the technique to predict the mode locations pretty well. The second option, saturation of MSA with respect to the accumulation mode, could explain the observed MSA distribution. Whether this kind of saturation is feasible under atmospheric conditions will be

discussed in the following subsection. Next the interaction between cloud processing and accumulation-mode particles is considered.

As demonstrated by both laboratory experiments and theoretical calculations, no more than one or two non-precipitating cloud cycles are needed to transfer an Aitken particle into the accumulation mode (Hoppel et al., 1994b; Kerminen and Wexler, 1995). When achieving the accumulation size, the growth of a residual particle (a particle that is left when water is taken away from the droplet) rapidly decelerates. Hence, successive cloud cycles shift small accumulation-mode particles toward larger ones, but cannot increase their diameter by more than a factor 2–3. As a result of cloud cycling, a condensate distributed initially according to the effective surface area of the accumulation mode will come closer to the mode's volume moment. This shows that processing of particles through clouds may, at least to some extent, be responsible for the observed distribution of MSA over the accumulation mode.

Cloud processing has other implications, too. The mass mean diameter of nss-SO_4^{2-} in the accumulation mode ranged from 0.31 to 0.48 μm in our samples. The accumulation-mode particles were relatively acidic in this study, and as such are expected to be aqueous over the observed *rh* range, 46–99% (see Potukuchi and Wexler, 1995). Since in addition no correlation between the average relative humidity and the mass mean diameter of the mode could be found, it can be claimed with some confidence that neither crystallization/deliquescence of the particles nor their growth/shrinkage due to changes in ambient *rh* can explain the variation of the mean size of the accumulation mode. A more probable explanation is that different samples had accumulated different amounts of sulfate during nonprecipitating cloud stages. This is supported by the greatest nss-SO_4^{2-} concentrations in samples #1, 2 and 5 having the greatest mass mean diameters for nss-SO_4^{2-}. One must bear in mind, however, that factors like a presence of different-size primary particles may contribute to the exact location of a mode.

3.6. *Saturation of MSA over the accumulation mode*

The possible saturation of MSA over the accumulation mode is worth exploring because it affects the distribution of MSA over the particle size range. The solubility of MSA in pure water is several orders of magnitude greater than that of nitric or hydrochloric acid, but clearly smaller than that of sulfuric acid (Clegg and Brimblecombe, 1985; Hoppel, 1987). Eisele and Tanner (1993) measured the evolution of gaseous MSA and H_2SO_4 concentrations during evening times, when the photochemical formation of these species is low. They found several incidences where the concentration of H_2SO_4(g) declined much more rapidly than that of MSA(g), indicating slower gas-to-particle transport for MSA. Only logical explanations for this phenomenon are that either MSA vapor had much lower accommodation coefficient on particle surfaces than H_2SO_4, or that the particulate phase was near its saturation with respect to MSA.

In mixed solutions, MSA solubility decreases rapidly with increasing acidity of the solution (e.g. Van Dingenen and Raes, 1993). Therefore, MSA should saturate more easily over the accumulation mode than over more alkaline sea-salt and soil particles. In our samples, the distributions of MSA and ammonium over the accumulation mode were quite similar. Since ammonia is the primary compound to neutralize submicron sulfate, this might have resulted from the saturation of MSA over particles of smaller ammonium content.

If MSA is near its saturation with respect to the accumulation mode, one would expect a certain fraction of it to evaporate from the impactor's low-pressure stages during the sampling (Zhang and McMurry, 1991). Our BLPI samples had some 10 to 30% lower MSA concentrations than the respective filter samples. This deviation does probably not result from differences in particle collection efficiencies between the two instruments, or from errors in chemical analyses, since concentrations of non-volatile species like sodium were quite similar for these two sampling methods. Thus, unless MSA is somehow destroyed in impactor samples prior to analysis, the deviation is likely to be due to evaporation of MSA during the sampling.

The above arguments give strong, albeit indirect, support for the saturation of MSA over the accumulation mode in the atmosphere. How does this affect the overall MSA size distribution? When accumulation-mode particles become saturated, they cannot absorb MSA any more, while the

supermicrometer particles probably can. Consequently, the amount of MSA in supermicron particles increases with respect to that in the accumulation mode.

Since MSA solubility is likely to be smaller for more acidic particles and for higher ambient temperatures, the saturation effect and subsequent supermicron enrichment of MSA are expected to occur primarily in environments that are warm and have a low ammonium to sulfate ratio. The available field data supports this view: at coastal or high-latitude sites some 80–90% of MSA commonly is associated with accumulation-mode particles (Salzman et al., 1983; Pszenny et al., 1989; Bergin et al., 1995; Leck and Persson, 1996), whereas over low-latitude marine oceans, a large fraction of it is found in the supermicron size range (Pszenny, 1992; Huebert et al., 1993).

4. Summary and conclusions

Formation of particulate MSA was studied by conducting a field campaign in the Finnish Arctic during the summer, 1995. The measurements involved size-segregated impactor sampling of MSA and major inorganic compounds, together with simultaneous monitoring of basic meteorological variables and aerosol parameters. Data interpretation was assisted by calculating 96-hour back trajectories for the measured air masses. Impactor data were run through an inversion procedure to construct continuous mass size distributions for the measured compounds.

Regardless of the air mass origin, four MSA modes could be identified: an accumulation mode centered between 0.3–0.5 μm of particle aerodynamic diameter, two supermicrometer modes that peaked at 2–3 and 7–10 μm, respectively, and an Aitken mode below 0.1 μm. Most MSA was found in the accumulation mode (70–90%), with minor amounts left in the Aitken (3–10%), and in the lower- (5–15%) and upper-size (1–10%) supermicron modes.

In most samples, the lower-size supermicron MSA mode followed closely the effective surface area of sea-salt particles, indicating it originated primarily from the condensational transport of gaseous MSA onto sea-salt particles. The other supermicron mode was hypothesized to be formed via the reaction of MSA(g) with soil-derived particles. Soil particles may also explain the broad supermicron MSA distributions sometimes observed in land-based sites. Aitken- and accumulation-mode MSA was separated by a gap around the 0.1 μm indicative of cloud processing. Accumulation-mode MSA peaked at the same size as ammonium, and at slightly smaller size than nss-SO_4^{2-}.

The ratio of MSA to nss-SO_4^{2-} concentration, R, ranged from 2 to 34%, with most of this variation resulting from different degrees of anthropogenic perturbation in the measured air masses. The ratio was clearly the highest for Aitken-mode particles which, unlike larger particles, do commonly not accumulate sulfate during cloud events. The large MSA to nss-SO_4^{2-} ratio over the Aitken range indicates further that MSA and sulfate contribute with comparable magnitudes to the nuclei condensational growth, at least in high-latitudes during the summer. Thus, although MSA may not participate in new particle production, it may play significant role in the subsequent growth of these particles into the CCN size. The evident variation of R with the particle size, together with potential enhanced MSA production in air influenced by pollution, demonstrate further that one needs to be extremely careful when using observed MSA to nss-SO_4^{2-} ratios in estimating the contribution of biogenic sources to total particulate sulfate in different environments.

The similar distributions of MSA and ammonium over the accumulation mode, like also the suspected partial evaporation of MSA from the impactor, suggest indirectly that MSA was near its saturation (chemical equilibrium between the gas and particulate phases) with respect to accumulation-mode particles. Saturation drives more MSA into the supermicrometer particles, especially for acidic aerosol systems at high temperatures. The saturation effect is a potential explanation for the general observation, according to which most MSA in coastal or high-latitude sites has usually been found in submicron particles, whereas over tropical oceans a significant fraction of MSA seems to be associated with supermicron particles.

The formation of submicrometer MSA is strongly tied with cloud processing. Interaction of air with nonprecipitating clouds moves particles from the Aitken mode into the accumulation mode, generates a gap between these two modes, and produces sulfate in the accumulation mode. Via changing the size and chemical composition of

accumulation-mode particles, this last phenomenon dictates to large extent how much MSA can be transported to the accumulation mode, and how it is distributed between this and the other modes.

5. Acknowledgements

This study was supported by the Academy of Finland and by the Maj and Tor Nessling Foundation.

REFERENCES

Andreae, M. O. and Raemdonck, H. 1983. Dimethyl sulphide in the surface ocean and the marine atmosphere: a global view. *Science* **221**, 744–747.

Ayers, G. P. and Gras, J. L. 1991. Seasonal relationship between cloud condensation nuclei and aerosol methanesulfonate in marine air. *Nature* **353**, 834–835.

Bandy, A. R., Scott, D. L., Blomquist, B. W., Chen, S. M. and Thornton, D. C. 1992. Low yields of SO_2 from dimethyl sulfide oxidation in the marine boundary layer. *Geophys. Res. Lett.* **19**, 1125–1127.

Bates, T. S., Calhoun, J. A. and Quinn, P. K. 1992. Variations in the methanesulfonate to sulfate molar ratio in submicrometer marine aerosol particles over the South Pacific Ocean. *J. Geophys. Res.* **97**, 9859–9865.

Bergin, M. H., Jaffrezo, J.-L., Davidson, C. I., Dibb, J. E., Pandis, S. N., Hillamo, R. E., Maenhaut, W., Kuhns, H. D. and Mäkelä, T. 1995. The contributions of snow, fog, and dry deposition to the summer flux of anions and cations at Summit, Greenland. *J. Geophys. Res.* **100**, 16275–16288.

Berner, A. and Lürzer, C. 1980. Mass size distributions of traffic aerosols in Vienna. *J. Phys. Chem.* **84**, 2079–2083.

Berresheim, H., Andreae, M. O., Iverson, R. L. and Li, S.-M. 1991. Seasonal variations of dimethylsulfide emissions and atmospheric sulfur and nitrogen species over the western north Atlantic Ocean. *Tellus* **43B**, 353–372.

Berresheim, H., Eisele, F. L., Tanner, D. J., McInnes, L. M., Ramsey-Bell, D. C. and Covert, D. S. 1993. Atmospheric sulfur chemistry and cloud condensation nuclei (CCN) concentrations over the northeastern Pacific coast. *J. Geophys. Res.* **98**, 12701–12711.

Bürgemeister, S. and Georgii, H.-W. 1991. Distribution of methanesulfonate, nss sulfate and dimethylsulfide over the Atlantic and the North Sea. *Atmos. Environ.* **25A**, 587–595.

Charlson, R. J., Lovelock, J. E., Andreae, M. O. and Warren, S. G. 1987. Oceanic phytoplankton, atmospheric sulfur, cloud albedo and climate. *Nature* **326**, 655–661.

Clegg, S. L. and Brimblecombe, P. 1985. The solubility of methanesulfonic acid and its implication for atmospheric chemistry. *Envir.Technol. Lett.* **6**, 269–278.

Eisele, F. L. and Tanner, D. J. 1993. Measurement of gas phase concentration of H_2SO_4 and methane sulfonic acid and estimates of H_2SO_4 production and loss in the atmosphere. *J. Geophys. Res.* **98**, 9001–9010.

Heintzenberg, J. and Leck, C. 1994. Seasonal variation of the atmospheric aerosol near the top of the marine boundary layer over Spitsbergen related to the Arctic sulphur cycle. *Tellus* **46B**, 52–67.

Hillamo, R. E. and Kauppinen, E. I. 1991. On the performance of Berner low pressure impactor. *Aerosol Sci. Technol.* **14**, 33–47.

Hoppel, W. A. 1987. Nucleation in the MSA-water vapor system. *Atmos. Environ.* **21**, 2703–2709.

Hoppel, W. A., Frick, G. M., Fitzgerald, J. W. and Larson, R. E. 1994a. Marine boundary layer measurements of new particle formation and the effects nonprecipitating clouds have on aerosol size distribution. *J. Geophys. Res.*, **99**, 14443–14459.

Hoppel, W. A., Frick, G. M., Fitzgerald, J. W. and Larson, R. E. 1994b. A cloud chamber study of the effect that nonprecipitating water clouds have on aerosol size distribution. *Aerosol Sci. Technol.* **20**, 1–30.

Huebert, B. J., Howell, S., Laj, P., Johnson, J. E., Bates, T. S., Quinn, P. K., Yegorov, V., Clarke, A. D. and Porter, J. N. 1993. Observations of the atmospheric sulfur cycle on SAGA 3. *J. Geophys. Res.* **98**, 16985–16995.

Jaffrezo, J.-L., Davidson, C. I., Legrand, M. and Dibb, J. E. 1994. Sulfate and MSA in the air and snow on the Greenland ice sheet. *J. Geophys. Res.* **99**, 1241–1253.

Kerminen, V.-M. and Wexler, A. S. 1995. Growth laws for atmospheric aerosol particles: An examination of the bimodality of the accumulation mode. *Atmos. Environ.* **29**, 3263–3275.

Koga, S. and Tanaka, H. 1993. Numerical study of the oxidation process of dimethylsulfide in the marine atmosphere. *J. Atmos. Chem.* **17**, 201–228.

Langner, J. and Rodhe, H. 1991. A global three-dimensional model of the tropospheric sulfur cycle. *J. Atmos. Chem.* **13**, 225–263.

Leck, C. and Persson, C. 1996. Seasonal and short-term variability in dimethyl sulfide, sulfur dioxide, and biogenic sulfur and sea salt aerosol particles in the Arctic marine boundary layer. *Tellus* **48B**, 272–299.

Lee, Y.-N. and Zhou, X. 1994. Aqueous reaction kinetics of ozone and dimethylsulfide and its atmospheric implications. *J. Geophys. Res.* **99**, 3597–3605.

Li, S.-M. and Barrie, L. A. 1993. Biogenic sulfur aerosol in the Arctic troposphere: 1. Contributions to total sulfate. *J. Geophys. Res.* **98**, 20613–20622.

Li, S.-M., Barrie, L. A., Talbot, R. W., Harris, R. C., Davidson, C. I. and Jaffrezo, J.-L. 1993. Seasonal and

geographic variations of methanesulfonic acid in the Arctic troposphere. *Atmos. Environ.* **27A**, 3011–3024.

Liu, B. Y. H. and Pui, D. Y. H. 1981. Aerosol sampling inlets and inhalable particles. *Atmos. Environ.* **15**, 589–600.

Mihalopoulos, M., Nguen, B. C., Boissard, C., Campin, J. M., Putaud, J. P., Belviso, S., Barnes, I. and Becker, K. H. 1992. Field study of dimethylsulfide oxidation in the boundary layer: variations of dimethylsulfide, methanesulfonic acid, sulfur dioxide, non-sea-salt sulfate and Aitken nuclei at a coastal Newman, L. 1981. Atmospheric oxidation of sulfur dioxide: a review as viewed from power plant and smelter plume studies. *Atmos. Environ.* **15**, 2231–2239.

Penner, J. E., Charlson, R. J., Hales, J. M., Laulainen, N. S., Leifer, R., Novakov, T., Ogren, J., Radke, L. F., Schwartz, S. E. and Travis, L. 1994. Quantifying and minimizing uncertainty of climate forcing by anthropogenic aerosols. *Bull. Am. Meteorol. Soc.* **75**, 375–400.

Potukuchi, S. and Wexler, A. S. 1995. Identifying solid-aqueous-phase transitions in atmospheric aerosols. II. Acidic solutions. *Atmos. Environ.* **29**, 3357–3364.

Pszenny, A. A. P. 1992. Particle size distributions of methanesulfonate in the tropical Pacific marine boundary layer. *J. Atmos. Chem.* **14**, 273–284.

Pszenny, A. A. P., Castelle, A. J., Galloway, J. N. and Duce, R. A. 1989. A study of the sulfur cycle in the Antarctic marine boundary layer. *J. Geophys. Res.* **94**, 9818–9830.

Quinn, P. K., Covert, D. S., Bates, T. S., Kapustin, V. N., Ramsey-Bell, D. C. and McInnes, L. M. 1993. Dimethylsulfide/cloud condensation nuclei/climate system: Relevant size-resolved measurements of the chemical and physical properties of atmospheric aerosol particles. *J. Geophys. Res.* **98**, 10411–10427.

Raes, F. 1995. Entrainment of free tropospheric aerosols as a regulating mechanism for cloud condensation nuclei in the remote marine boundary layer. *J. Geophys. Res.* **100**, 2893–2903.

Russell, L. M., Pandis, S. N. and Seinfeld, J. H. 1994. Aerosol production and growth in the marine boundary layer. *J. Geophys. Res.* **99**, 20989–21003.

Saltelli, A. and Hjorth, J. 1995. Uncertainty and sensitivity analyses of OH-initiated dimethyl sulfide (DMS) oxidation kinetics. *J. Atmos. Chem.* **21**, 187–221.

Salzman, E. S., Savoie, D. L., Zika, R. G. and Prospero, J. M. 1983. Methane sulfonic acid in the marine atmosphere. *J. Geophys. Res.* **88**, 10897–10902.

Saltzman, E. S., Savoie, D. L., Prospero, J. M. and Zika, R. G. 1986. Methanesulfonic acid and non-sea-salt sulfate in Pacific air: Regional and seasonal variations. *J. Atmos. Chem.* **4**, 227–240.

Savoie, D. L., Prospero, J. M., Larsen, R. J. and Saltzman, E. S. 1992. Nitrogen and sulfur species in aerosols at Mawson, Antarctica, and their relationship to natural radionuclides. *J. Atmos. Chem.* **14**, 181–204.

Valkama, I. and Rossi, J. 1992. Description of the model TRADOS. In: *Evaluation of long range atmospheric transport model using environmental radioactivity data from the Chernobyl accident. The ATMES Report* (ed. by Klug W., Graziani G., Grippa Van Dingenen, R. and Raes, F. 1993. Ternary nucleation of methanesulfonic acid, sulphuric acid and water vapor. *J. Aerosol Sci.* **24**, 1–17.

Wang, H. C. and John W. 1988. Characteristics of the Berner impactor for sampling inorganic ions. *Aerosol Sci. Technol.* **8**, 157–172.

Watts, S. F., Brimblecombe, P. and Watson A. J. 1990. Methanesulphonic acid, dimethyl sulfoxide and dimethyl sulphone in aerosols. *Atmos. Environ.* **24A**, 353–359.

Winklmayr W., Wang, H.-C. and John, W. 1988. Adaption of the Twomey algorithm to the inversion of cascade impactor data. *Aerosol. Sci. Technol.* **13**, 322–331.

Wolfenbarger, J. K. and Seinfeld, J. H. 1990. Inversion of aerosol size distribution data. *J. Aerosol Sci.* **21**, 227–247.

Zhang, X. and McMurry, P. H. 1991. Theoretical analysis of evaporative losses of adsorbed or absorbed species during atmospheric aerosol sampling. *Environ. Sci. Technol.* **25**, 456–459.